

# Investigation of a Machine learning methodology for the SKA pulsar search pipeline

Shashank Sanjay Bhat<sup>1\*</sup>, Prabu Thiagaraj<sup>2</sup>, Ben Stappers<sup>3</sup>, Atul Ghalame<sup>3</sup>, Snehanishu Saha<sup>4</sup>, T.S.B Sudarshan<sup>5</sup>, Zaffirah Hosenie<sup>3</sup>

<sup>1</sup>During the work affiliated to Raman Research Institute, Bangalore, India

<sup>\*</sup>Now with IBM India Private Ltd, Bangalore, India

<sup>2</sup>Raman Research Institute, Bangalore, India

<sup>3</sup>University of Manchester, Manchester

<sup>4</sup>APPCAIR, BITS Goa, Goa - 403726, India

<sup>5</sup>PES University, Bangalore, India

<sup>\*</sup>Corresponding author. E-mail: ssbhat98@gmail.com

**Abstract.** The SKA pulsar search pipeline will be used for real time detection of pulsars. Modern radio telescopes such as SKA will be generating petabytes of data in their full scale of operation. Hence experience-based and data-driven algorithms become indispensable for applications such as candidate detection. Here we describe our findings from testing a state of the art object detection algorithm called Mask R-CNN to detect candidate signatures in the SKA pulsar search pipeline. We have trained the Mask R-CNN model to detect candidate images. A custom annotation tool was developed to mark the regions of interest in large datasets efficiently. We have successfully demonstrated this algorithm by detecting candidate signatures on a simulation dataset. The paper presents details of this work with a highlight on the future prospects.

**Keywords.** Modern Radio Telescopes—Anomaly Detection—Time Series—Mask R-CNN—Binary pulsars.

## 1. Introduction

Modern Radio Telescopes such as the Square Kilometre Array (SKA) generate data in the order of petabytes in their full scale of operation. Data volumes arise due to the extensive array size (197 antennas in South Africa and 1,31,072 antennas in Western Australia), multiple beams (up to about 1500), broadband digitisation (about 800 Msps), and from the demanding science requirements (1, 2015; Dewdney *et al.*, 2015). Correspondingly there is considerable high-speed signal processing: FFT, filtering, cross-correlations, beam-forming, etc., employed using dedicated hardware components. Subsequent processing uses a mix of application-specific and non-deterministic algorithms, where statistical and experience-based decision making is indispensable.

Manual or semi-automated approaches will not be feasible when handling such volumes of data. We will have to employ automated and heuristic algorithms that can ease the classification of data, detection of patterns/objects in the data streams in real-time. Machine Learning, which is an actively evolving field, brings in a host of valuable practical techniques to efficiently han-

dle the radio-telescope large volume data processing.

This paper investigates the use of a state of the art object detection module called Mask R-CNN in order to detect accelerated binary pulsar signatures in an incoming data stream present in the pulsar search pipeline. In the previous efforts by (Lyon *et al.*, 2016; Keith *et al.*, 2010; Bates *et al.*, 2012) candidate detection was performed after the pulsar profiles were obtained. We demonstrate a novel approach of detecting candidate signatures in the middle of the processing pipeline. Additionally our effort for detecting binary pulsar signatures involving machine learning based approaches is novel. By determining the location, coordinates of the candidate we will be able to extract useful information from the data which will be beneficial to the pulsar search.

This paper is outlined as follows: Section 2. gives a brief background on machine learning. Section 3. introduces the SKA pulsar search pipeline (Levin *et al.*, 2017), the Fourier Domain Acceleration Search (FDAS)(Ransom, 2001) and the machine learning pipeline which was investigated. Section 4. provides a discussion about the challenges faced in the modern radio telescopes due to Radio frequency Inter-

ference and provides a proposal which can be applied to SKA and other SKA Era telescopes.

## 2. Background on Machine Learning

Machine Learning is the study of algorithms which can improve over time with experience and data. Machine Learning is classified into three categories : 1. Supervised Learning, 2. Unsupervised Learning and 3. Reinforcement Learning.

The term Supervised Learning implies that the data is labeled. An Artificial Intelligence (AI) model creates a mapping between the features and output and uses this mapping function to predict values for new datasets. Support Vector Machines (Hearst *et al.*, 1998), Decision Trees (Quinlan, 1986), K-Nearest Neighbors (Cunningham & Delany, 2022) are some of the widely used supervised machine learning algorithms.

Unsupervised machine learning signifies Artificial Intelligence (AI) models which creates a mapping function by clustering and grouping similar data. K-means clustering (Jain, 2008), Expectation Maximization clustering (Moon, 1996), Auto encoders (Bank *et al.*, 2020) are some of the widely used unsupervised machine learning algorithms.

Reinforcement Learning works on the concept of an Artificial Intelligence (AI) agent which observes its surroundings and performs an action. Based on the action taken it is either rewarded or penalized (Sutton, 2005). Over time the AI model will aim towards maximizing the reward function.

In most of the above three categories of machine learning the underlying workhorse is a neural network. A neural network is primarily composed of neurons (Gurney, 1997). A neuron takes a sum of weighted inputs along with a bias and subjects this output to an activation function. The activation function determines if a neuron has to switch on or off. Figure 1 shows a general structure of a neuron with two inputs and a bias.

In some of the problems present in astronomy we apply neural network based approaches to create the mapping between the input data and its corresponding labels. Neural networks can be effectively used for modeling the behaviour of a function. But in case of complex functions more number of neurons in the form of layers will have to be added. A neural network with multiple hidden layers is called a deep neural network. Figure 2 shows an artificial neural network with one hidden layer.

In case of pulsar searches we will have to deal with large amounts of image based data and the processing will have to be done in real time (Lyon *et al.*, 2018). Lyon et al, 2018 in their paper introduces a real time

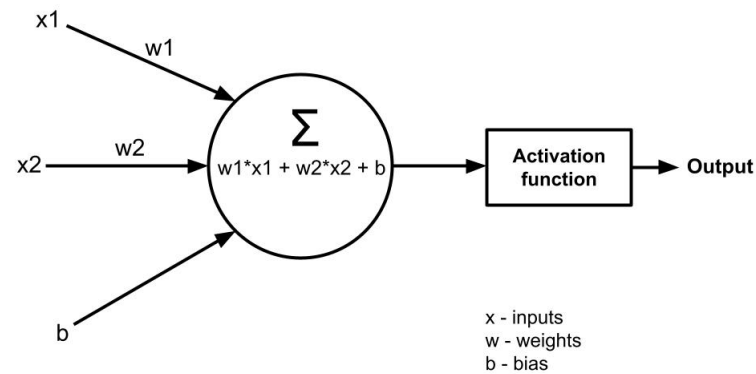


**Figure 1.** The structure of an artificial neuron having two inputs, two weights, a bias and an activation function

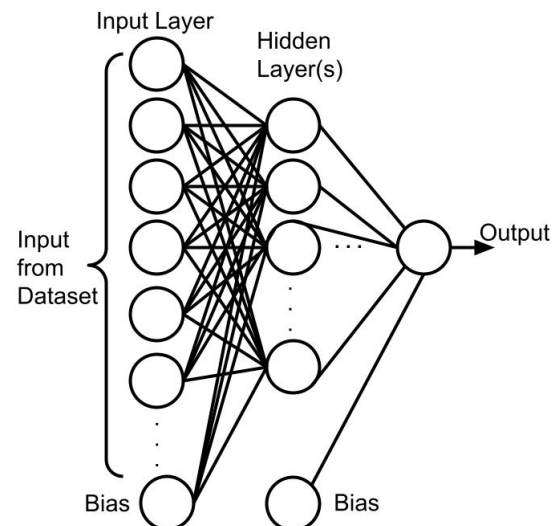


**Figure 2.** An Artificial Neural network having multiple neurons, one input layer, one hidden layer and one output. For complex problems the neural network can have multiple hidden layers. For multi class classification problems there are multiple neurons in the output layer.

pulsar candidate detection pipeline.

When dealing with image data we use a special case of an Artificial Neural Network called the Convolutional Neural Network (CNN) (Krizhevsky *et al.*, 2012). The feature extraction in a CNN happens with a repeated set of convolutions and pooling. Convolutions are performed via filters to produce feature maps. The pooling layer is responsible for reducing the spatial size of the feature maps. This additionally helps in reducing the computation power required. The extracted features are then fed into a series of neurons which then perform classification.

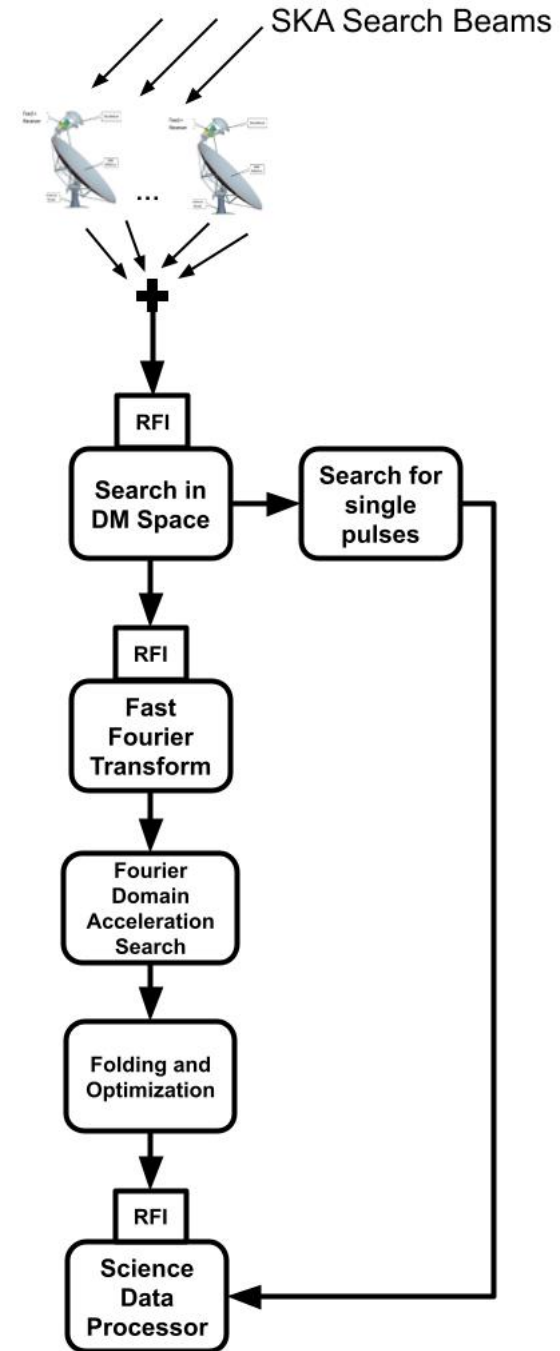
### 3. SKA Pulsar Search pipeline

Figure 3 shows the pulsar search pipeline which will be used at SKA. Our focus is on the Fourier Domain Acceleration Search module. We have investigated the effectiveness of Mask R-CNN to detect candidates of accelerated binary pulsar signatures.

#### 3.1 Fourier Domain Acceleration Search

The intermediate product of the Fourier Domain Acceleration Search (FDAS) module when viewed as a particular image intensity mode a distinct shape (Hourglass, Butterfly) is observed. The intensity, location and inclination of these shape / patterns give us information about these candidates.

We found that basic image processing algorithms to detect the intensity patterns would not be feasible for images having relatively low SNR (Signal to Noise Ratio). Additionally, basic CNNs (Convolutional Neural Network) could perform classification very effectively but they would not be useful in our case as they could not draw a bounding box around the classified object. A bounding box is necessary in our case for determining the co-ordinates of the candidate. Convolution based methods are very efficient for template matching although computationally expensive to implement. In our case due to the use of accelerators additional computation steps for implementing convolutions is less significant. The R-CNN and Fast R-CNN algorithm (Girshick, 2015) which uses a selective search algorithm could not be used for real life deployments as there was a performance bottleneck. The Faster R-CNN algorithm (Ren *et al.*, 2015) could not be used as we needed a mask to be drawn for every detected object. Due to these reasons we chose Mask R-CNN to perform candidate signature detection. Our investigation is to see if the Mask R-CNN suite can be used to train and recognize these image patterns. We have identified the public domain availability of Mask R-CNN from matterport



**Figure 3.** Schematic of the pulsar search processing work flow in SKA. FPGA based acceleration architecture investigated for 1) RFI mitigation, 2) dedispersion, 3) FFT, 4) acceleration search and 5) candidate folding optimisation modules.

github repository.([Repository Link](#))<sup>1</sup>

### 3.2 Mask R-CNN

Mask R-CNN (He *et al.*, 2017) is a small, flexible generic object instance segmentation framework. It not only detects targets in the image, but also gives a high-quality segmentation result for each target. It is extended on the basis of Faster R-CNN, and adds a new branch for predicting an object mask which is parallel with bounding box recognition branch. For object classification we have used the default ResNet101 (He *et al.*, 2015) as our classification network. For the Detection network, we have used a Region Proposal Network which was proposed with the Faster R-CNN algorithm. Feature Extraction in the Mask R-CNN happens via the Feature Pyramid Network (FPN) algorithm. The FPN algorithm was designed to handle images of various sizes and shapes by keeping speed, memory and accuracy in mind. The algorithm consists of both a top down and bottom up approach for producing feature maps. The bottom up network features a regular convolutional neural network for extracting features from images. Every layer in the bottom up pyramid reduces spatially allowing for high level structures to be determined, thereby increasing the semantic value. The top down network provides a pathway to construct high resolution layers from the semantic rich layer. Additionally there are lateral connections provided to help the detector better detect the object locations. This algorithm has shown significant improvements over the other state-of-the-art approaches (Lin *et al.*, 2016). Mask R-CNN defines the loss function as follows:

$$L = L_{cls} + L_{box} + L_{mask} \quad (1)$$

Where  $L_{cls}$  denotes the classification loss,  $L_{box}$  denotes the bounding box loss and  $L_{mask}$  is the average binary cross entropy loss, only including k-th mask if the region is associated with the ground truth class k.

### 3.3 Basic Tests with Mask R-CNN

Mask R-CNN is available as a github repository from matterport. The github repository is cloned onto our local system following the setup procedure given in the github repository

By default Mask R-CNN has been pretrained on 80 different objects from the MS COCO (Lin *et al.*, 2014) dataset. Figure 4 is an example of the default detection by the Mask R-CNN on a city image. In addition, in order to understand the training procedure of

Mask R-CNN we have experimented it to detect damages in car images. For this purpose we collected sample images from an external github repository ([Repository Link](#))<sup>2</sup>. It was required to annotate the images using Visual Geometry Group (VGG) annotator. We then trained the Mask R-CNN suite using the standard procedures described in github. The loss function for this experiment remains the same as the standard loss function described in section 3.2. For this experiment we haven't performed any predictive success analysis. Figure 5 shows the result from training Mask R-CNN on the car damage dataset.

The training of the neural network is an important task and this procedure is described in the next section.

### 3.4 Training a neural network

Every neural network requires a good dataset (both qualitatively and quantitatively). A dataset is split into three parts i.e., a training set which is used in the neural network, a validation set which is used for preventing overfitting and a testing set to evaluate the performance of a neural network. During the training of the neural network there is a specific loss function which is defined. A loss function can either be predetermined or a custom user defined. The loss function gives us an approximate idea about how well an algorithm models a given data. A neural network updates its weights with the backpropagation algorithm. A forward pass in a neural network is defined as one run starting from the input layer until the output layer. A combination of one forward propagation and one backward propagation is called an epoch. During the training cycle the algorithm is subjected to the training data and is validated with the validation dataset. When the validation loss begins exceeding the training loss we can safely conclude the training process and extract the weights. The weights are a crucial database produced at the end of the training process which will help in making appropriate connection between the neurons. The weights will be provided to the inferencing logic.

### 3.5 Adapting Mask R-CNN for candidate detection

As discussed before, The default Mask R-CNN is used for detecting generic objects. We will have to train the Mask R-CNN to produce a new set of weights for detecting the candidate signatures (hourglass/butterfly patterns). This process involves four steps :

- Preparing the dataset

<sup>1</sup>[https://github.com/matterport/Mask\\_RCNN](https://github.com/matterport/Mask_RCNN)

<sup>2</sup>[https://github.com/priya-dwivedi/Deep-Learning/tree/master/mask\\_rcnn\\_damage\\_detection/customImages](https://github.com/priya-dwivedi/Deep-Learning/tree/master/mask_rcnn_damage_detection/customImages)



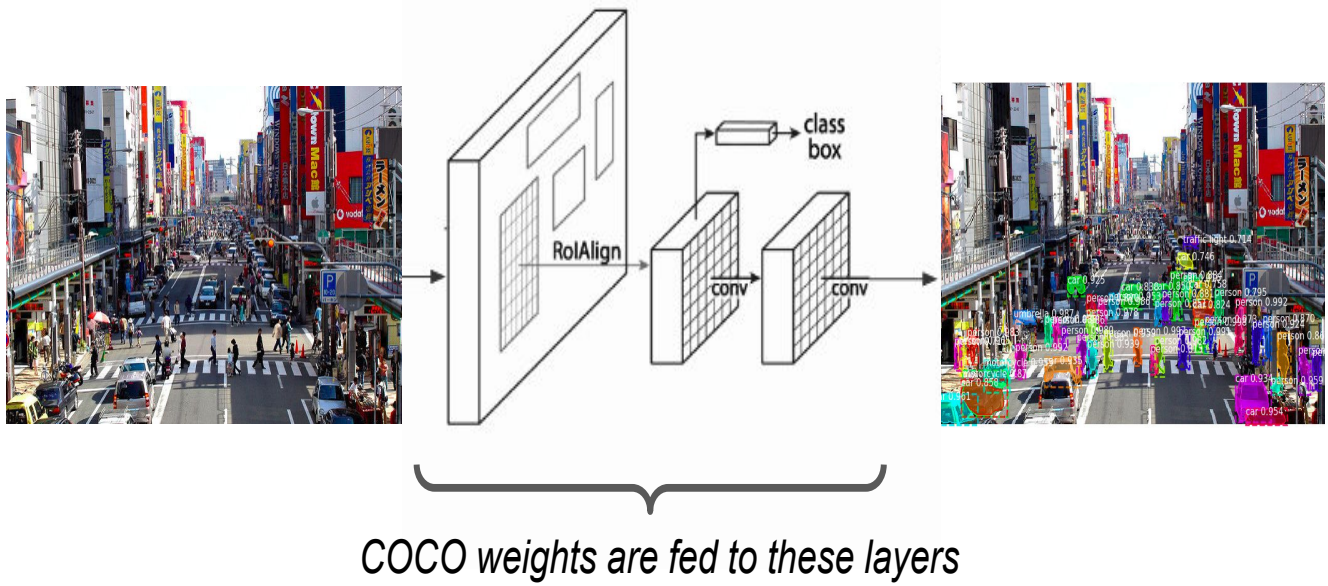


**Figure 4.** As a basic step we took the default MS-COCO weights along with Mask R-CNN. MS-COCO weights are provided along with the Mask R-CNN repository. A city image was taken and subjected to this algorithm. We observed that to one extent of the resolution of the image it could detect objects, draw bounding boxes on each of the detected along with a confidence score and additionally draw a mask for each of the detected objects.



**Figure 5.** Before getting into candidate detection, we trained Mask R-CNN on a custom car damage dataset. Input images along with their respective masks were taken as input to the model. The custom weights were extracted and were tested on test images. This figure shows the result on one of the test images which was taken.

**Figure 6.** This figure shows the ideal input and output scenario for a candidate signature image. The custom dataset will be annotated and then trained on Mask R-CNN in order to get a custom weights file. This weights file will be used for detecting signatures on a new set of test images.

- Image Annotation
- Training
- Testing

### 3.6 Preparing the Dataset

We considered to use simulated pulsar datasets that are conventionally used for testing the pulsar search pipeline. This file contained 536 seconds of observation data. The dataset is subjected to Fast Fourier Transform followed by a set of filtering operations to get a Filter Output Plane : a two dimensional array of 85 by 4 mil-

lion. For SNR optimization across the search parameter space the authors have found the set of 85 filters to be required to search across pulsar periods up to 500 Hz with  $\pm 350 \text{ ms}^{-2}$  acceleration arising due to their orbital motions. A typical sample lengths of 4 M samples corresponds an observation time of about 10 minutes (Thiagaraj *et al.*, 2020). To extract the images from the 85 by 4 million data array we have used a combination of a sliding window approach at selected regions where there are more likelihood presence of signals and noise (starting from fundamental frequency to multiple harmonic positions). Figure 7 shows the images obtained by processing multiple datasets having varying Signal strength (Signal to Noise Ratio). For this study we con-

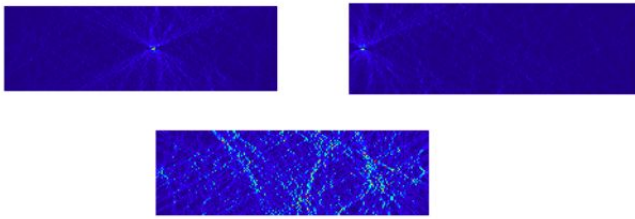


**Figure 7.** The first image on the top left shows a candidate image with a high intensity. We have taken the size of the image to be  $85 * 256$  pixels. The candidate signatures in the shape of a butterfly are obtained after subjecting the candidate array to 85 different acceleration filters. The second image in the top right shows the same candidate but it is shifted to the corner. The third image in the bottom shows the candidate image dominated with noise.

sidered 38 simulation files and produced 886 segments from the original Filter Output Plane. Some of these segments had the butterfly pattern. After removing the images with complete noise we were left with 309 images. The removal of images with complete noise was performed via a combination of visual inspection and our existing knowledge of analyzing data through conventional FFT and filtering algorithms. As a first step we have considered only 50 images with the highest clarity to train the Mask R-CNN model.

### 3.7 Image Annotation

The Mask R-CNN model requires annotating the images using the VGG tool. Initially we have used the standard VGG tool for annotation subsequently we have developed our own annotator that worked faster and helps in annotating large datasets.

**3.7.1 Image annotation using VGG Annotator** VGG Annotator developed by the visual geometry group allows for high precision masking. We annotated our 50 image dataset manually using a six point reference for the mask and saved the co-ordinates in a json format. The only drawback with this method is the time which is taken for a significantly larger dataset. Due to this drawback we developed a solution to perform semi-automated annotation. Figure 8 shows the mask drawn using VGG Annotator.

**3.7.2 Image Annotation using Custom Annotator** The same set of 50 images were annotated using our semi-automated approach. The custom annotator was primarily developed to reduce the amount of human effort during annotation of the dataset. Our semi-automated solution also draws a six point reference



**Figure 8.** A candidate image with a high SNR is taken and is subjected to a tool named VGG Annotator (Visual Geometry Group). The figure above shows the image being superimposed by a mask drawn on the VGG tool.



**Figure 9.** The same candidate image with a high SNR is taken and is subjected to a custom tool which was developed in-house. Our custom tool draws the mask by only taking the center bright dot as the reference point. The figure above shows the mask drawn by our custom annotator tool over the candidate image.

mask with respect to a central point chosen by the end user. In our case the six point reference mask is calculated mathematically with respect to the central point. We found the time taken for annotating a larger dataset is significantly lower with our custom annotator. Figure 9 shows the mask drawn by the custom annotator.

### 3.8 Training

While performing the training we have configured the model to save the weights file at every epoch. For the dataset at hand we set the total epochs to be 6. The loss curves are an indicator to show when the training has completed. The same dataset is fed to the network a few times in order to build an effective mapping function for the weights. Typically the flattening of the loss curve implies that the training can be terminated. In Figure 10 we can observe that after epoch 2 the loss curves are flattening. It can also be observed that two of our annotation methods (VGG and Custom Annotator) have shown similar results. Since the loss curves started flattening at the second epoch we terminated our training process at the third epoch. We utilized transfer learning to train our Mask R-CNN suite for three epochs. The pretrained COCO weights were used as the base weights file in the training. The model was trained with a learning rate of 0.001 on both VGG annotated datasets and custom annotated datasets. The learning rate is a tuning parameter that determines the step size

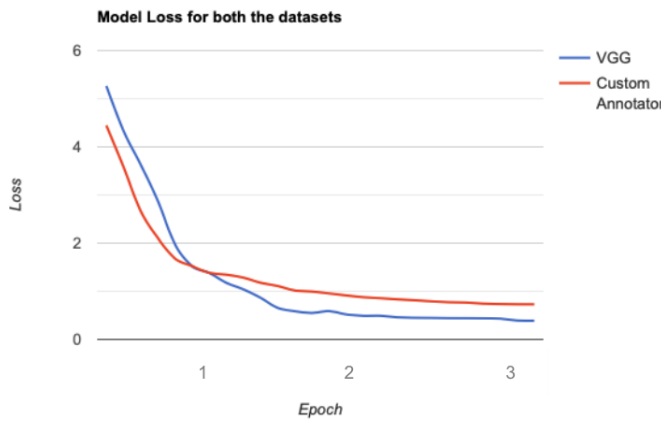


**Figure 10.** We subjected the Mask R-CNN model to train on 50 high resolution images. These images were annotated with both VGG Annotator and our custom developed annotator. This figure shows the loss curves achieved for both the datasets when trained for 3 epochs.

at each iteration while moving toward a minimum of a loss function. A larger learning rate signifies a higher chance of convergence at a local minima. A smaller learning rate signifies a higher chance of convergence at a global minima.

The training is compute intensive and we have used Google Colab which is equipped with a Nvidia T4 GPU. Mask R-CNN has a specific configurable parameter which is known as `IMAGES_PER_GPU`. We found that by limiting the number of images to be processed by the GPU to 2 the computation was faster. We have also made the training process to accept images if the confidence score is above 90 percent. Figure 10 shows the model loss curves for both the datasets.

### 3.9 Results from our experiment

After the training process we obtained two weight files (i.e., one for the VGG annotated dataset and another for the custom annotated dataset) and passed it onto the Mask R-CNN inferencing logic. We subjected the inferencing logic on 8 test images. Among these 8 images we took 4 images to be the highest SNR (Signal to Noise Ratio), 2 to be having medium SNR and 2 to be having low SNR. Among the 4 high SNR images which were taken, 2 images with the candidate signature in the centre and 2 towards the corners.

**3.9.1 VGG Annotator results** The images with centred candidate signatures gave us a single detected object with an extremely high confidence score along with the mask. The candidate signatures towards the corner gave us multiple detections with the candidate having

the highest confidence score but the mask was not being drawn at the right place. The medium SNR images had only candidate signatures in the centre. The trained model gave multiple detections with the candidate having the highest confidence score but the mask was drawn at the right place in this case. For the low SNR images there were multiple false detections with low confidence scores and in specific cases there were no detections which were found in the images. For the weights obtained on the VGG annotated.

**3.9.2 Custom Annotator Results** We considered the same 8 images for the custom annotator as well. The high SNR ones in this case had multiple detections regardless of the candidate signature location. The medium SNR images also gave multiple detected objects and the actual candidate signature had the highest confidence score. The low SNR cases gave multiple detections each with a low confidence score and in specific cases there were no detections. In each of the cases the mask was not drawn over the detected objects.

Figures 11 and 12 show the results obtained from the Mask R-CNN. In each of the figures the bounding boxes signify the detected objects by the Mask R-CNN model. Each of these bounding boxes have their respective confidence scores. Figure 11 provides a visual depiction of the results for 2 test images. These images are a part of the 8 images which were taken up for testing as described in subsection 3.9.1. In this case we can observe the mask drawn for the bounding box with the highest confidence score. In the case of Figure 12 the same set of images are tested with the Mask R-CNN model trained on custom annotated images. In this case we observe that the size of the bounding boxes have reduced in comparison to the VGG annotator results. Additionally, the detected bounding boxes have no mask drawn in them.

## 4. Discussion on Future Perspectives

The current design of SKA pulsar search is likely to use machine learning approaches for RFI detection and pulsar candidate identification. As described by Lyon et al, these are well tested approaches. We have investigated a new machine learning approach for another intermediate stage in the search processing (FDAS) where candidate detection is routinely performed using numerical methods. The present Mask R-CNN pipeline test reports only detection. By including code features to determine the location, inclination and intensity of the candidates more information can be passed on to the candidate sifting logic (Sorting). Thus the pipeline can



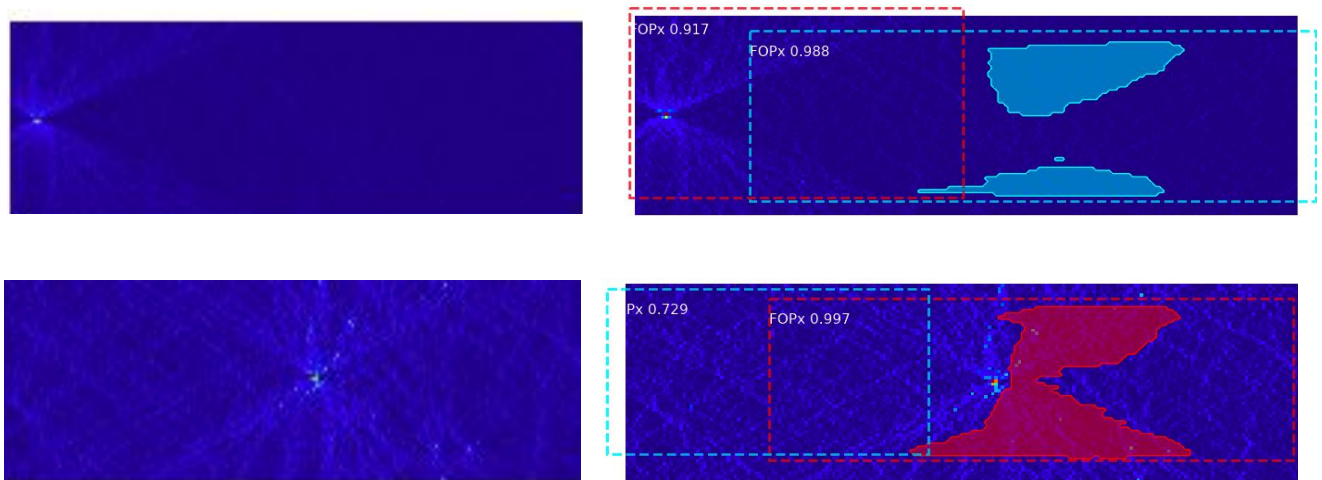


**Figure 11.** The training of the Mask R-CNN model in both the cases gave rise to two weight files. One weight file was obtained for the VGG annotated dataset and another weight file was obtained for the custom annotator. This figure shows the results on two test images subjected to the Mask R-CNN model with the VGG Annotated weights. Here we consider two scenarios, one of the images having the candidate signature in the corner and another one having the candidate signature in the center. The Mask R-CNN model draws a bounding box over the detected objects along with a mask. Each of the bounding boxes have a confidence score which is present.

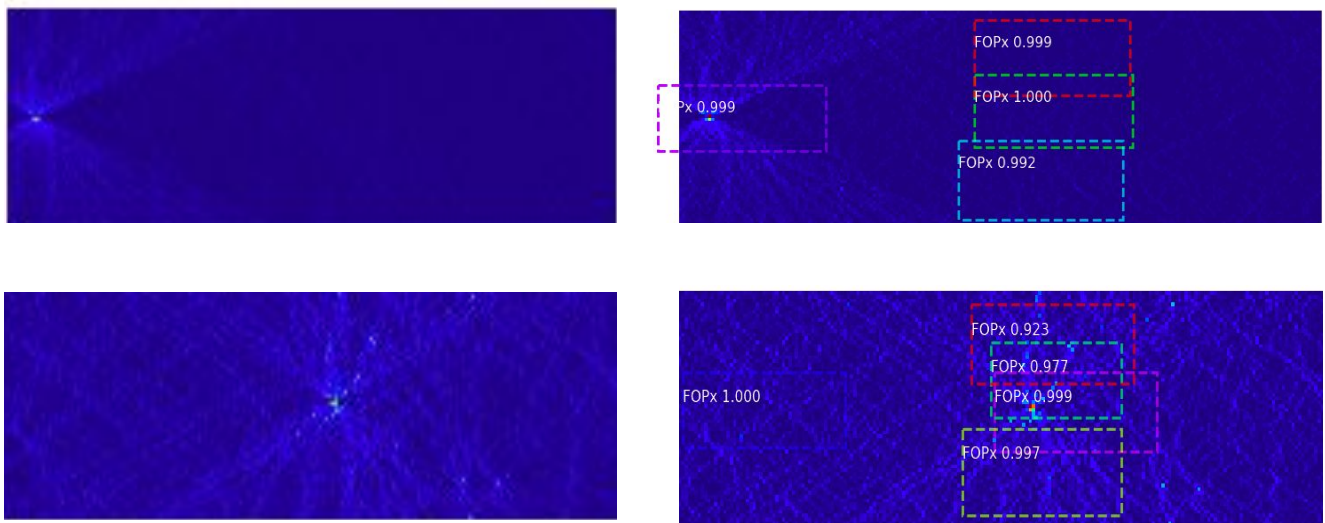


**Figure 12.** This figure shows the results on two test images subjected to the Mask R-CNN model with the custom annotated weights. Here we consider same set of images as above i.e., one of the images having the candidate signature in the corner and another one having the candidate signature in the center. The Mask R-CNN model in this case detects multiple objects in the image. The size of the bounding box is smaller when in comparison to the VGG results. Additionally, we observe that there is no mask present in either of the scenarios.

be improved to provide higher level of information during the search.

Since this is a new method, the implementation schemes and their interfaces with successive stages needs to be further explored. For this purpose we have investigated the use of FPGA platform and OpenCL languages. We have carried out a study for hardware ac-

celeration of Mask R-CNN for future implementation. Since the pulsar search pipeline runs on an accelerator, we have studied the possibility of running the Mask R-CNN algorithm on FPGA platforms. In our early investigation we found the OpenCL porting of Mask R-CNN is achievable. However more work needs to be done to map the different libraries used by Mask R-



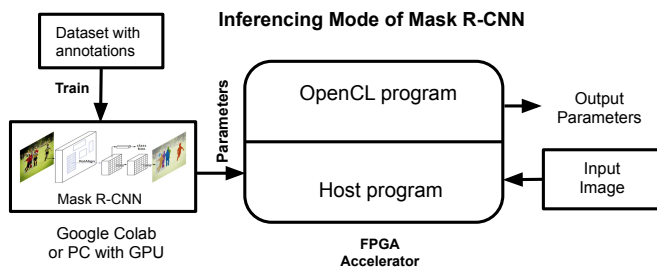


**Figure 13.** This figure shows how a Mask R-CNN acceleration could be done for an FPGA based deployment. The Mask R-CNN will get trained on a GPU/CPU based device and will then be converted into OpenCL equivalent code which can execute instructions parallelly. The host code will handle the basic input and output of an image.

CNN. Proposed implementation of Mask R-CNN for hardware is shown in Figure 13.

Additionally, every modern radio telescope data analysis faces challenges in the form of Radio Frequency Interference.

We found that the concept of Radio Frequency Interference can be looked at as a time series problem. We wanted to use Time series machine learning models on the same database to determine whether a future observation slot will be free from interference or not. The task can be split into two parts: Part 1 can use unsupervised machine learning algorithms such as K-means clustering and EM clustering to detect signal anomalies in the form of Radio Frequency Interference (RFI) in the incoming radio stream. Prior to clustering the statistical properties such as Kurtosis and Skew (Misra *et al.*, 2007, 2008) of a radio signal can be used to extract features for the classification. A simple testing of this idea can be performed using a software defined radio (RTL-SDR) based data collection. Our experimentation showed that K-means clustering and Expectation Maximization clustering were effective. In the second part of the work LSTM (Long Short Term Memory) based techniques can be used to predict predicting short term trends (Bhat *et al.*, 2020).

## 5. Conclusion and Future Work

The paper showed the potential of a machine learning algorithm Mask R-CNN for detecting candidate images in a pulsar search pipeline. Our results from testing Mask R-CNN are very encouraging. We have used high clarity images to train the Mask R-CNN model. However, the model was able to detect images with lower intensities as well successfully. Additionally, we have

also developed a custom annotator tool to mark the regions of interest for the image annotation. We have discussed about the difficulties in handling data in the presence of RFI. We have also discussed future prospects of this work.

## Acknowledgements

The authors would like to thank Raman Research Institute, University of Manchester, PES University and BITS Goa for their support.

## References

- 1, S. P. 2015, SKA PHASE 1 EXECUTIVE SUMMARY, [https://www.skatelescope.org/wp-content/uploads/2021/03/22380\\_SKA\\_Project-Summary\\_v4\\_single-pages.pdf](https://www.skatelescope.org/wp-content/uploads/2021/03/22380_SKA_Project-Summary_v4_single-pages.pdf)
- Bank, D., Koenigstein, N., & Giryas, R. 2020, Autoencoders, doi:10.48550/ARXIV.2003.05991
- Bates, S. D., Bailes, M., Barsdell, B. R., *et al.* 2012, Monthly Notices of the Royal Astronomical Society, 427, 1052
- Bhat, S. S., Prabu, T., & Saha, S. 2020, 2020 XXXIIIrd General Assembly and Scientific Symposium of the International Union of Radio Science, 1
- Cunningham, P., & Delany, S. J. 2022, ACM Computing Surveys, 54, 1
- Dewdney, P., Turner, W., Braun, R., *et al.* 2015, SKA1 SYSTEM BASELINEV2 DESCRIPTION, [https://www.skatelescope.org/wp-content/uploads/2014/03/SKA-TEL-SKO-0000308\\_SKA1\\_System\\_Baseline\\_v2\\_DescriptionRev01-part-1-signed.pdf](https://www.skatelescope.org/wp-content/uploads/2014/03/SKA-TEL-SKO-0000308_SKA1_System_Baseline_v2_DescriptionRev01-part-1-signed.pdf)
- Girshick, R. 2015, Fast R-CNN, doi:10.48550/ARXIV.1504.08083
- Gurney, K. 1997, An Introduction to neural Networks, [https://www.inf.ed.ac.uk/teaching/courses/nlu/assets/reading/Gurney\\_et\\_al.pdf](https://www.inf.ed.ac.uk/teaching/courses/nlu/assets/reading/Gurney_et_al.pdf)
- He, K., Gkioxari, G., Dollár, P., & Girshick, R. 2017, Mask R-CNN, doi:10.48550/ARXIV.1703.06870
- He, K., Zhang, X., Ren, S., & Sun, J. 2015, Deep Residual Learning for Image Recognition, doi:10.48550/ARXIV.1512.03385

- Hearst, M., Dumais, S., Osuna, E., Platt, J., & Scholkopf, B. 1998, IEEE Intelligent Systems and their Applications, 13, 18
- Jain, A. K. 2008, in Machine Learning and Knowledge Discovery in Databases, ed. W. Daelemans, B. Goethals, & K. Morik (Berlin, Heidelberg: Springer Berlin Heidelberg), 3–4
- Keith, M. J., Jameson, A., Straten, W. V., *et al.* 2010, Monthly Notices of the Royal Astronomical Society, 409, 619
- Krizhevsky, A., Sutskever, I., & Hinton, G. E. 2012, in Advances in Neural Information Processing Systems 25, ed. F. Pereira, C. J. C. Burges, L. Bottou, & K. Q. Weinberger (Curran Associates, Inc.), 1097–1105
- Levin, L., Armour, W., Baffa, C., *et al.* 2017, Proceedings of the International Astronomical Union, 13, 171
- Lin, T.-Y., Dollár, P., Girshick, R., *et al.* 2016, Feature Pyramid Networks for Object Detection, doi:10.48550/ARXIV.1612.03144
- Lin, T.-Y., Maire, M., Belongie, S., *et al.* 2014, Microsoft COCO: Common Objects in Context, doi:10.48550/ARXIV.1405.0312
- Lyon, R. J., Stappers, B. W., Cooper, S., Brooke, J. M., & Knowles, J. D. 2016, Monthly Notices of the Royal Astronomical Society, 459, 1104
- Lyon, R. J., Stappers, B. W., Levin, L., Mickaliger, M. B., & Scaife, A. 2018, A Processing Pipeline for High Volume Pulsar Data Streams, doi:10.48550/ARXIV.1810.06012
- Misra, S., Kristensen, S. S., Søbjaerg, S. S., & Skou, N. 2007, 2007 IEEE International Geoscience and Remote Sensing Symposium, 2714
- Misra, S., Ruf, C., & Kroodsma, R. 2008, in IGARSS 2008 - 2008 IEEE International Geoscience and Remote Sensing Symposium, Vol. 2, II–335–II–338
- Moon, T. 1996, IEEE Signal Processing Magazine, 13, 47
- Quinlan, J. R. 1986, Induction of Decision Trees, <https://www.hunch.net/~coms-4771/quinlan.pdf>
- Ransom, S. M. 2001, Fast Search Techniques for High Energy Pulsars, doi:10.48550/ARXIV.ASTRO-PH/0112006
- Ren, S., He, K., Girshick, R., & Sun, J. 2015, Faster R-CNN: Towards Real-Time Object Detection with Region Proposal Networks, doi:10.48550/ARXIV.1506.01497
- Sutton, R. S. 2005, History of Reinforcement Learning, <http://www.incompleteideas.net/book/ebook/node12.html>
- Thiagaraj, P., Stappers, B., Ghalame, A., *et al.* 2020, in 2020 XXXIIIrd General Assembly and Scientific Symposium of the International Union of Radio Science, IEEE, 1–5